

BBA 42586

## Functional size measurements on the chloroplast cytochrome *bf* complex

Jonathan H.A. Nugent and Derek S. Bendall

Department of Botany and Microbiology, University College London, London, and Department of Biochemistry,  
University of Cambridge, Cambridge (U.K.)

(Received 22 January 1987)

**Key words:** Radiation inactivation; Cytochrome *bf* complex; Rieske iron-sulphur protein; Chloroplast membrane; Electron transfer; (*P. sativum*)

Radiation inactivation studies on the functional size of the chloroplast cytochrome *bf* complex showed the following characteristics. (1) In the purified complex, the cytochrome *b*-563, cytochrome *f* and Rieske polypeptides gave independent target sizes close to those obtained from gene sequence data. (2) The molecular mass required for electron transport from plastoquinol-1 to plastocyanin in chloroplast membranes was approximately 75 kDa. This indicates that one copy of each major polypeptide forms a functional complex. (3) Measurements on the Rieske EPR signal indicate that the binding of the inhibitor 2,5-dibromo-6-methyl-3-isopropyl-*p*-benzoquinone (DBMIB) involves more than one polypeptide. It is argued that the quinone-binding site blocked by DBMIB involves both the Rieske and cytochrome *b* polypeptides.

### Introduction

Chloroplast cytochrome *bf* complex isolated from thylakoid membranes is one of a family of oxidoreductases which are also found in the electron transport systems of mitochondria and bacteria [1–3]. Cytochrome *bf* complex catalyses the oxidation of plastoquinol by plastocyanin, which involves both electron and proton transport across the thylakoid membrane and facilitates electron transfer between the two photosystems. The membrane-bound complex contains four major polypeptides and several redox centres: (a)

cytochrome *b*-563, 23.4 kDa (spinach) containing two *b*-type haem groups [4]; (b) cytochrome *f*, 31.1 kDa (pea) containing a *c*-type haem group [5,6]; (c) a Rieske-type iron-sulphur protein, 18.9 kDa (spinach; Herrmann, R.G., personal communication); (d) plastoquinone/ol bound to one or more proteins [7]; (e) a 15.2 kDa (pea) polypeptide of unknown function [8] which is related to the C terminus of the larger mitochondrial cytochrome *b*. This suggests that the cytochrome *b* in chloroplasts is a split gene [9].

The molecular mass of each major polypeptide has been derived from gene sequence data and does not include the electron carriers associated with the polypeptide. As with the membrane proteins of the *Rhodospseudomonas viridis* reaction centre [10], it demonstrates that molecular size data based on SDS-polyacrylamide gel electrophoresis can contain large over- or underestimations.

Models of possible structures for the four poly-

Abbreviations: DBMIB, 2,5-dibromo-6-methyl-3-isopropyl-*p*-benzoquinone; Mes, 4-morpholineethanesulphonic acid; Chl, chlorophyll; SDS, sodium dodecyl sulphate; PS, Photosystem.

Correspondence: J.H.A. Nugent, Department of Botany and Microbiology, University College London, Gower Street, London, WC1E 6BT, U.K.

peptides indicate that they all span the membrane and these models also allow suggestions for the location of some electron carriers [3,9]. However, the mechanism of electron and proton transport remains to be firmly established. 'Q' and 'b' cycle models involving the two *b* cytochromes and also a quinone-binding site on either side of the membrane have been suggested (see Refs. 1–3 for review).

Knowledge of the number and stoichiometry of the major polypeptides is important to the understanding of the structure and function of the complex. Many techniques including quantitative staining or radioactive labelling of SDS-polyacrylamide gels, cross-linking and binding studies, light scattering, gel filtration, sedimentation and electron microscopy [1–3,11–17] have been applied to cytochrome *bc* type complexes. No agreement has been reached on either the stoichiometry or number of individual polypeptides.

Radiation inactivation measures the functional size of proteins and protein complexes [18–21]. The rate of loss of activity with increasing radiation dose is measured. If activity declines as a single exponential function of dose, a linear plot of dose versus log activity is obtained. The slope of this plot is related to the molecular mass by calibration using enzymes of known molecular mass [20]. The technique is particular suitable for membrane-bound protein complexes, which are often difficult to purify. Using this technique, purification is only required to the stage where the characteristic or activity can be accurately measured. However, the interpretation of results can be complicated by the presence of detergents, which may affect rates of inactivation [20].

This paper reports an investigation of the cytochrome *bf* complex using radiation inactivation. Measurements were made on both purified complex and chloroplast membranes. The rate of electron transport from plastoquinol to plastocyanin was used to measure overall electron transport, and the site of DBMIB binding was investigated using the characteristic shift of the EPR spectrum of the Rieske iron-sulphur centre. The results indicate that a monomeric complex of subunits is active and that the binding site for DBMIB involves more than one polypeptide.

## Materials and Methods

Chloroplast membranes were prepared from the leaves of greenhouse-grown peas (*Pisum sativum*, var. Feltham First) by the method described in Ref. 22 and were suspended in 20 mM Mes/15 mM NaCl/5 mM MgCl<sub>2</sub>/20% (v/v) glycerol. Purified cytochrome *bf* complex was prepared by the method of Hurt and Hauska [23]. Samples were prepared for radiation treatment as described in Ref. 19 and irradiated in the presence of enzyme standards, malate dehydrogenase (70 kDa) and glucose-6-phosphate dehydrogenase (104 kDa), as described in Ref. 20. The use of bovine serum albumin was avoided, due to the reversal of DBMIB inhibition by this protein [24]. 0.5 mg/ml transferrin was used in place of bovine serum albumin as a protein buffer. Radiation treatment was carried out at a dose rate of 2 Mrad per min as detailed in Refs. 20 and 21. Samples irradiated at room temperature were cooled during treatment using air driven over a block cooled by liquid nitrogen. Treatment was given in a series of 4-Mrad doses with a cooling period between each, until the required dose was achieved.

Irradiation was carried out at 77 K using samples in quartz glass tubes immersed in liquid nitrogen contained in a finger dewar. Treatment was given in 15- or 20-Mrad doses until the required dose was achieved.

## Assays

Chlorophyll *a* and *b* were measured by the method of Arnon [25] using 80% (v/v) acetone. Enzymes were assayed at either 20 or 25°C using duplicate or triplicate assays of each sample. Temperature variation was  $\pm 0.5^\circ\text{C}$  and could be corrected for by using control samples. Enzyme assays were as described in Ref. 20 using a Cary 219 spectrophotometer and 1 ml, 1 cm pathlength quartz cuvettes. Malate dehydrogenase (porcine heart cytoplasmic, EC 1.1.1.37) was assayed by the rate of oxidation of NADH monitored at 340 nm, using freshly made oxaloacetate solution as substrate. Glucose-6-phosphate dehydrogenase from *Leuconostoc mesenteroides* (EC 1.1.1.49) was assayed by the rate of reduction of NAD<sup>+</sup>, monitored at 340 nm using glucose 6-phosphate as substrate. The Rieske iron-sulphur protein was

estimated using the size of the EPR signal at  $g = 1.89$  and the effect of DBMIB by the height of the modified Rieske EPR signal at  $g = 1.95$ . Cytochromes *b* and *f* were measured as the height of the absorption peaks at 563 and 554 nm in a reduced-minus-oxidised (ferricyanide) optical difference spectrum using automatic baseline correction. The cytochrome *f* peak was obtained by reduction with hydroquinone and checked by further reduction with sodium ascorbate. The cytochrome *b*-563 peak was obtained by subtraction of the cytochrome *f* peak from a sodium dithionite-minus-ferricyanide difference spectrum.

Plastoquinol/plastocyanin oxidoreductase activity was measured by following the reduction of plastocyanin at 579 nm [26]. The reaction mixture contained 20 mM Mes (pH 6.2)/80 mM NaCl/10  $\mu$ M plastocyanin/10  $\mu$ M plastoquinol-1/0.1% digitonin and chloroplasts (5  $\mu$ g chlorophyll) in a total volume of 1 ml. After addition of digitonin, the suspension was incubated for 2 min before adding plastoquinol to start the reaction. Rates were corrected for the uncatalysed rate observed in the absence of chloroplasts (about 10%). Pea plastocyanin was purified by the method of Plesnicar and Bendall [27] and plastoquinol-1 was synthesised as described in Ref. 26.

#### EPR spectrometry

EPR spectrometry was performed at cryogenic temperatures using a Jeol FE1 X-band spectrometer with 100 kHz field modulation and an Oxford instruments liquid helium cryostat. 0.3-ml samples in 3 mm diameter calibrated quartz tubes were used. Chlorophyll concentration of samples and EPR conditions are described in the text. Samples were prepared as follows. (a) Rieske iron-sulphur centre: 10 mM sodium ascorbate was added to samples, which were then dark adapted for 15–20 min before freezing in liquid nitrogen in the dark. This treatment reduces the Rieske centre but not the iron-sulphur centres which act as PS I electron acceptors. (b) DBMIB/Rieske centre; samples were prepared with addition of 100  $\mu$ M DBMIB and after 15 min of dark adaptation were frozen under illumination from a 1000 W lamp. Samples were examined by EPR at 15 K, the measurement of the size of EPR signals is described in the text.

#### Data analysis

A Minitab statistical programme (Penn State University) was used for linear regression and analysis of variance. Enzyme activities were expressed as a percentage of control values and target analysis performed as in Refs. 19 and 20. Regression lines were checked for error by a plot of standard residuals versus dose. Molecular mass was estimated by comparison with the protein standards [20,21]. Errors, expressed as S.D., were approximately  $\pm 10\%$ . A Tectronix 4051 microcomputer was used to store EPR spectra.

#### Results

The rates of inactivation of the electron carriers were first established using data from the absorption spectra of cytochromes *b* and *f* and EPR spectra of the Rieske iron-sulphur centre. The purified cytochrome *bf* complex was investigated by radiation inactivation of freeze-dried samples. Fig. 1 shows in a single experiment the inactivation of the Rieske centre compared to the enzyme standards malate dehydrogenase and glucose-6-phosphate dehydrogenase. Comparison of the rate of inactivation of the Rieske centre with the standards gave a molecular mass of 19 kDa with malate dehydrogenase and 17 kDa with glucose-

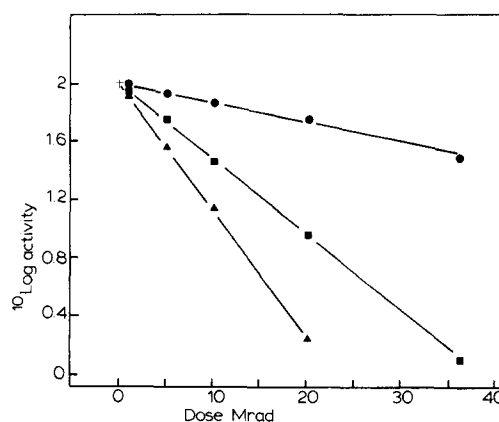


Fig. 1. Rate of inactivation of the Rieske centre in the cytochrome *bf* complex. Freeze-dried samples were irradiated at room temperature and assays performed as given in materials and methods. ●, Rieske iron-sulphur centre ( $g = 1.89$ ); ■, malate dehydrogenase; ▲, glucose-6-phosphate dehydrogenase. Slopes of regression lines ( $\text{Mrad}^{-1}$ ): ●,  $(1.41 \pm 0.05) \cdot 10^{-2}$ ; ■,  $(5.28 \pm 0.07) \cdot 10^{-2}$ ; ▲,  $(8.77 \pm 0.12) \cdot 10^{-2}$ .

6-phosphate dehydrogenase. This compares favourably with the mass from sequence data (18.9 kDa) and shows the accuracy of measurement from a single experiment to be approximately  $\pm 10\%$ . Similar comparisons for cytochrome *b* and *f* (not shown) were made and gave molecular sizes of 25 kDa (cytochrome *b*) and 30 kDa (cytochrome *f*), indicating that the inactivation was a function of the whole molecule. The size of the individual targets for these three polypeptides which carry most if not all of the electron transfer components suggests that the overall functional size of the complex could be measured.

Chloroplast membranes irradiated at 77 K were used to measure oxidoreductase activity. This avoided the presence of detergents, which have been shown to affect molecular size estimations [20]. Fig. 2A and B shows the rates of inactivation of malate dehydrogenase and plastoquinol-1/plastocyanin oxidoreductase activity compared to the Rieske iron-sulphur centre in chloroplast membrane samples. The results of two separate experiments using identical conditions were combined to increase the accuracy of measurement.

The rate of inactivation of chlorophyll was used as a baseline (molecular weight, 1000) to subtract secondary inactivation processes. Subtraction of the chlorophyll inactivation from that of Rieske centre, malate dehydrogenase and oxidoreductase produces rates showing that the inactivation of the oxidoreductase was more than three times that of the Rieske centre. The rate of inactivation of the oxidoreductase activity was also very similar to that of malate dehydrogenase. These comparisons indicate a molecular size of around 75 kDa for oxidoreductase activity using plastoquinol-1. This is similar to the combined molecular masses of the cytochromes *b* and *f* plus the Rieske polypeptide. It shows that a monomeric arrangement of polypeptides is functionally competent and, with an accuracy of  $\pm 10\%$ , indicates that the 15 kDa polypeptide may have no functional role.

#### DBMIB

The effect of DBMIB binding on the rate of inactivation of the Rieske centre was measured using the change in EPR characteristics. Conditions were established which allowed full conversion of the normal Rieske EPR signal to the signal

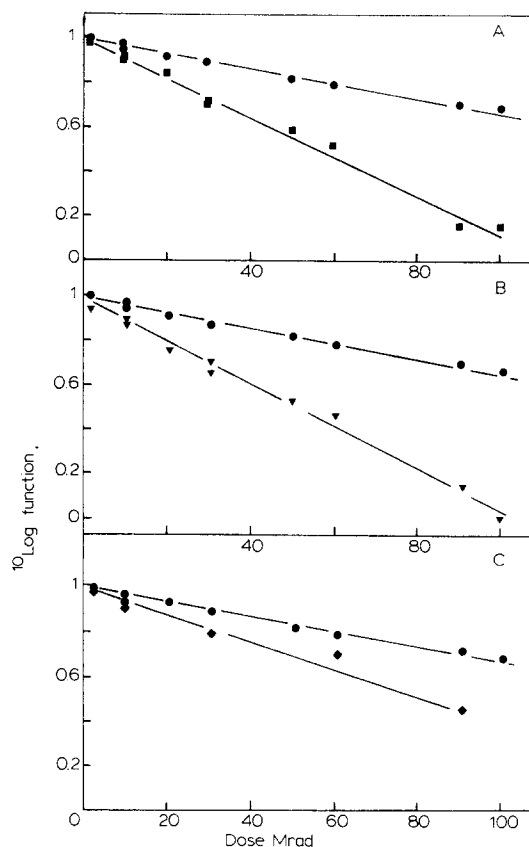


Fig. 2. Rate of inactivation of cytochrome *bf* complex in chloroplast samples irradiated at 77 K. Comparison of the rates of inactivation of the Rieske centre ( $g = 1.89$ ) (●) with (A) malate dehydrogenase (■), (B) plastoquinol-1/plastocyanin oxidoreductase (▼) and (C) the  $g = 1.95$  signal caused by addition of  $100 \mu\text{M}$  DBMIB (◆). Results of two separate experiments are combined in A and B. EPR samples were prepared and measured as given in the text. Slopes of regression lines ( $\text{Mrad}^{-1}$ ) (each experiment): ■,  $3.2 \cdot 10^{-3}$  and  $3.15 \cdot 10^{-3}$ ; ■,  $9.2 \cdot 10^{-3}$  and  $8.4 \cdot 10^{-3}$ ; ▼,  $9.4 \cdot 10^{-3}$  and  $9.1 \cdot 10^{-3}$ ; ◆,  $5.8 \cdot 10^{-3}$ . Chlorophyll concentrations of the two experiments were 4 and  $1.75 \text{ mg/ml}$ . Rate of inactivation of chlorophyll,  $1.1 \cdot 10^{-3}$ .

caused by DBMIB interaction [28,29]. As demonstrated in Fig. 3, the addition of DBMIB to the ascorbate reduced cytochrome *bf* complex produced a variable mixture of signals from centres where DBMIB was bound ( $g = 1.95$ ) and not bound ( $g = 1.89$ ). It was found that reproducible conversion of the  $g = 1.89$  Rieske signal to the  $g = 1.95$  form could not be achieved using chemical reduction but occurred when chloroplast samples were frozen under illumination following

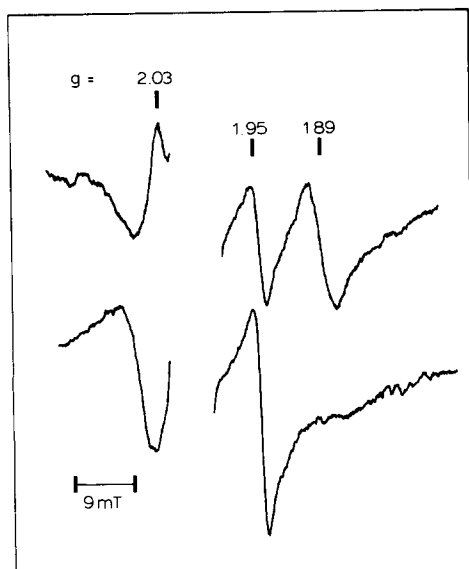


Fig. 3. EPR spectra of the Rieske iron-sulphur centre showing the effect of DBMIB. Both spectra are from chloroplast samples containing  $100 \mu\text{M}$  DBMIB and  $3 \text{ mg Chl/ml}$ . Upper line, sample reduced by  $10 \text{ mM}$  sodium ascorbate and frozen after  $15 \text{ min}$  dark adaptation. Lower line, sample frozen under illumination. The significance of the  $g$  values marked is given in the text.

DBMIB addition (Fig. 3, lower spectrum). Measurement of the rate of inactivation of the  $g = 1.95$  signal revealed a significantly increased rate as compared to that of the normal Rieske centre (Fig. 2C). Further experiments were performed on freeze-dried chloroplast membranes in order to obtain a greater rate of inactivation by using room temperature radiation treatment. Fig. 4 shows the results of two experiments. The upper graph shows the rate of inactivation of the  $g = 1.89$  'normal' Rieske signal together with the rate of inactivation of the standard malate dehydrogenase. The lower graph compares the rates of inactivation of the  $g = 1.89$  'normal' and  $g = 1.95$  DBMIB signals. There is a clear difference between the two rates, indicating a molecular size of around  $45\text{--}50 \text{ kDa}$  for the  $g = 1.95$  signal by comparison with  $70 \text{ kDa}$  for malate dehydrogenase and  $20 \text{ kDa}$  for the  $g = 1.89$  Rieske signal. This shows that the binding site for DBMIB is not solely the polypeptide of the Rieske centre. It suggests that binding occurs either on a polypeptide adjacent to the Rieske centre, which would still allow an interac-

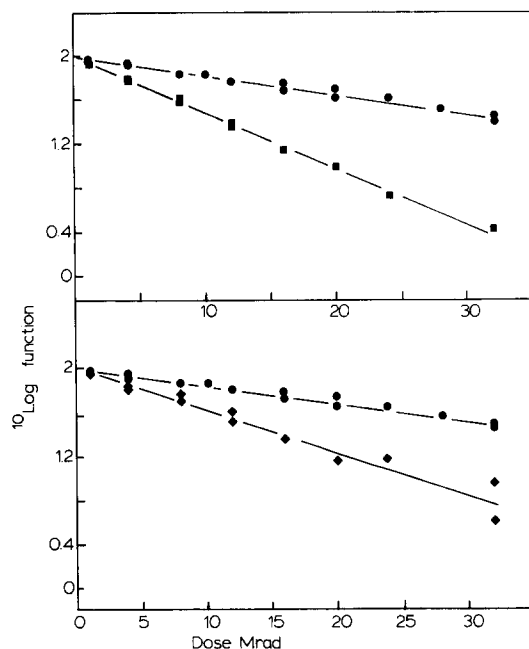


Fig. 4. Rate of inactivation of the  $g = 1.89$  and  $g = 1.95$  EPR signals from the cytochrome *bc* complex. Freeze-dried chloroplasts were irradiated at room temperature and samples prepared ( $3 \text{ mg Chl/ml}$ ) and assayed as given in Materials and Methods. Upper graph, comparison of the rates of inactivation of the  $g = 1.89$  Rieske EPR signal ( $\bullet$ ) and malate dehydrogenase ( $\blacksquare$ ). Lower graph, comparison of the rates of inactivation of the  $g = 1.89$  ( $\bullet$ ) and  $g = 1.95$  DBMIB ( $\blacklozenge$ ) EPR signals. The Rieske and malate dehydrogenase data are from three separate experiments and the DBMIB data from two experiments. Slopes of regression lines ( $\text{Mrad}^{-1}$ ) (each experiment):  $\bullet$ ,  $1.48 \cdot 10^{-2}$ ,  $1.56 \cdot 10^{-2}$  and  $1.76 \cdot 10^{-2}$ ;  $\blacksquare$ ,  $5.25 \cdot 10^{-2}$ ,  $4.9 \cdot 10^{-2}$  and  $6.2 \cdot 10^{-2}$ ;  $\blacklozenge$ ,  $3.45 \cdot 10^{-2}$  and  $4.4 \cdot 10^{-2}$ .

tion, or perhaps involves both the Rieske centre and an additional polypeptide(s).

## Discussion

Several recent publications have provided evidence that the cytochrome *bc*-type complexes function as dimers. These results have suggested that modifications are required to the hypotheses put forward to explain the mechanism of catalysis. According to the protonmotive Q cycle, the oxidoreductase contains two centres, one where plastoquinol is oxidised,  $\text{QO}$  (also designated  $\text{Q}_0$  or  $\text{Q}_z$ , see Refs. 1–3) and another for plastoquinone reduction,  $\text{QR}$  ( $\text{Q}_i$  or  $\text{Q}_c$ ). Two protons are released at  $\text{QO}$ , with one electron passed to

the Rieske iron-sulphur centre and the other passed across the membrane to the QR site. Two classes of inhibitor which independently block each of these proposed sites have been demonstrated. DBMIB inhibits at the QO site. The evidence for a dimeric complex has been used mainly to provide alternative explanations for the co-operative reduction of plastoquinone at the QR site, but a double Q cycle has also been proposed [13]. The strongest evidence for the existence of dimers comes from electron microscopy of mitochondrial cytochrome *bc* complex [12,17] and chloroplast cytochrome *bf* complex [16]. However, the functional unit could still be monomeric.

Nalecz and Azzi suggested that a monomer of mitochondrial cytochrome was active [15], but with the dimeric form having increased activity. Hurt and Hauska [23] also argued that the monomeric complex was active in their isolated cytochrome *bf* complex preparation.

Studies on inhibitor binding have indicated one binding site per complex for the mitochondrial inhibitors of QO, myxothiazol [30] and stigmatellin [31], suggesting a monomeric complex. On the other hand, Graan and Ort [11] recently suggested that there was only one DBMIB binding site per dimeric complex of cytochrome *bf*. Therefore, there is no consensus for the monomer or dimer model.

The results presented in this study clearly show that the cytochrome *bf* complex is a functional monomer for plastoquinol-1/plastocyanin oxidoreductase activity. This does leave the possibility that a slight enhancement of activity by dimerisation may occur. This should have caused a biphasic inactivation but may not have been resolved.

The binding site for DBMIB and plastoquinol has been suggested to be the Rieske iron-sulphur polypeptide because this centre is probably the electron acceptor at the QO site. Photoaffinity labelling of cytochrome *bf* complexes with plastoquinone analogues showed binding to the Rieske polypeptide but also binding to the cytochrome *b*, an effect which was reduced by DBMIB binding [7]. The competition between the artificial electron donor duroquinol and DBMIB has recently been investigated, with the results suggesting that they compete for the QO site [32].

The results presented here show that the DBMIB site involves more than the Rieske polypeptide. It is possible that the site does not involve the Rieske polypeptide at all, as its mass may only feature because of the use of the EPR signal for measurement of the DBMIB binding. However, the data taken together with the photoaffinity labelling results suggest that the DBMIB site, and therefore probably the QO site, depend on both the Rieske and cytochrome *b* polypeptide. Analysis of the amino acid sequence information for the cytochrome *b* [4,9] suggests that the most probable candidate for quinone binding would have to involve the conserved histidine residues involved in haem binding. The two quinone-binding sites may therefore occupy sites on either side of the membrane close to the cytochrome *b* haem groups.

### Acknowledgements

We thank the Nuffield Foundation for financial support. We also thank Keith Jordan for technical assistance and David Adams at Addenbrookes Hospital for help with the linear accelerator.

### References

- 1 Bendall, D.S. (1982) *Biochim. Biophys. Acta* 683, 119–152
- 2 Hauska, G., Hurt, E., Gabellini, N. and Lockau, W. (1983) *Biochim. Biophys. Acta* 726, 97–133
- 3 Murphy, D.J. (1986) *Biochim. Biophys. Acta* 864, 33–94
- 4 Widger, W.R., Cramer, W.A., Herrmann, R.G. and Trebst, A. (1984) *Proc. Natl. Acad. Sci. USA* 81, 674–678
- 5 Willey, D.L., Auffret, A.D. and Gray, J.C. (1984) *Cell* 36, 555–562
- 6 Alt, J. and Herrmann, R.G. (1984) *Curr. Genet.* 8, 551–557
- 7 Oettmeier, W., Masson, K., Soll, H.-J., Hurt, E. and Hauska, G. (1982) *FEBS Lett.* 144, 313–317
- 8 Phillips, A.L. and Gray, J.C. (1984) *Mol. Gen. Genet.* 194, 477–484
- 9 Cramer, W.A., Widger, W.R., Herrmann, R.G. and Trebst, A. (1985) *Trends Biochem. Sci.* 10, 125–129
- 10 Deisenhofer, J., Epp, O., Miki, K., Huber, R. and Michel, H. (1985) *Nature* 318, 618–624
- 11 Graan, T. and Ort, D.R. (1986) *Arch. Biochem. Biophys.* 248, 445–451
- 12 Leonard, K.R., Wingfield, P.A.T. and Weiss, H. (1981) *J. Mol. Biol.* 149, 259–274
- 13 De Vries, S., Albracht, S.P.J., Bearden, J.A. and Slater, E.C. (1982) *Biochim. Biophys. Acta* 681, 41–53
- 14 Nalecz, M.J., Bolli, R. and Azzi, A. (1985) *Arch. Biochem. Biophys.* 236, 619–628

- 15 Nalecz, M.J. and Azzi, A. (1985) *Arch. Biochem. Biophys.* 240, 921–931
- 16 Morschel, E. and Staehelin, L.A. (1983) *J. Cell Biol.* 97, 301–310
- 17 Linke, P., Bechmann, G., Gothe, A. and Weiss, H. (1986) *Eur. J. Biochem.* 158, 615–621
- 18 Kempner, E.S. and Schlegel, W. (1979) *Anal. Biochem.* 92, 2–10
- 19 Nugent, J.H.A. and Atkinson, Y.E. (1984) *FEBS Lett.* 170, 89–93
- 20 Nugent, J.H.A. (1986) *Biochem. J.* 239, 459–462
- 21 Nugent, J.H.A. (1987) *Biochim. Biophys. Acta* 890, 160–168
- 22 Ford, R.C. and Evans, M.C.W. (1983) *FEBS Lett.* 160, 159–164
- 23 Hurt, E. and Hauska, G. (1981) *Eur. J. Biochem.* 117, 591–599
- 24 Robinson, H.H., Guikema, J.A. and Yocum, C.F. (1980) *Arch. Biochem. Biophys.* 203, 687–690
- 25 Arnon, D.I. (1949) *Plant Physiol.* 24, 1–15
- 26 Wood, P.M. and Bendall, D.S. (1976) *Eur. J. Biochem.* 61, 337–344
- 27 Plesnicar, M. and Bendall, D.S. (1970) *Biochim. Biophys. Acta* 216, 192–199
- 28 Malkin, R. (1981) *FEBS Lett.* 131, 169–172
- 29 Malkin, R. (1982) *Biochemistry* 21, 2945–2950
- 30 Thierbach, G. and Reichenbach, H. (1981) *Biochim. Biophys. Acta* 638, 282–289
- 31 Thierbach, G., Kunze, B., Reichenbach, H. and Hoefle, G. (1984) *Biochim. Biophys. Acta* 765, 227–235
- 32 Nanba, M. and Katoh, S. (1986) *Biochim. Biophys. Acta* 851, 484–490